Bioconjugate Chemistry

Article

pubs.acs.org/bc

Stereochemistry of Amino Acid Spacers Determines the Pharmacokinetics of ^{111}In−DOTA−Minigastrin Analogues for Targeting the CCK2/Gastrin Receptor

Petra Kolenc Peitl,[†] MariaLuisa Tamma,[‡] Marko Kroselj,[†] Friederike Braun,[§] Beatrice Waser,[∥] Jean Claude Reubi,[∥] Marija Sollner Dolenc,[⊥] Helmut R. Maecke,[‡,§] and Rosalba Mansi*[,‡,§]

[†]Department of Nuclear Medicine, University Medical Centre Ljubljana, Zaloska cesta 7, SI-1000 Ljubljana, Slovenia

[‡]Division of Radiological Chemistry, University Hospital Basel, Petersgraben 4, CH-4031 Basel, Switzerland

[§]Department of Nuclear Medicine, University of Freiburg, Hugstetterstrasse 55, 79106 Freiburg, Germany

[∥]Division of Cell Biology and Experimental Cancer Research, Institute of Pathology, University of Berne, Murtenstrasse 31, CH-3010 Berne, Switzerland

[⊥]Faculty of Pharmacy, University of Ljubljana, Askerceva cesta 7, SI-1000 Ljubljana, Slovenia

Supporting Information

ABSTRACT: The metabolic instability and high kidney retention of minigastrin (MG) analogues hamper their suitability for use in peptide−receptor radionuclide therapy of CCK2/gastrin receptor-expressing tumors. High kidney retention has been related to N-terminal glutamic acids and can be substantially reduced by coinjection of polyglutamic acids or gelofusine. The aim of the present study was to investigate the influence of the stereochemistry of the N-terminal amino acid spacer on the enzymatic stability and pharmacokinetics of ^{111}In−DOTA−(D-Glu)$_6$-Ala-Tyr-Gly-Trp-Met-Asp-Phe-NH$_2$ (^{111}In−PP11−**D**) and ^{111}In−DOTA−(L-Glu)$_6$-Ala-Tyr-Gly-Trp-Met-Asp-Phe-NH$_2$ (^{111}In−PP11−**L**). Using circular dichroism measurements, we demonstrate the important role of secondary structure on the pharmacokinetics of the two MG analogues. The higher in vitro serum stability together with the improved tumor-to-kidney ratio of the (D-Glu)$_6$ congener indicates that this MG analogue might be a good candidate for further clinical study.

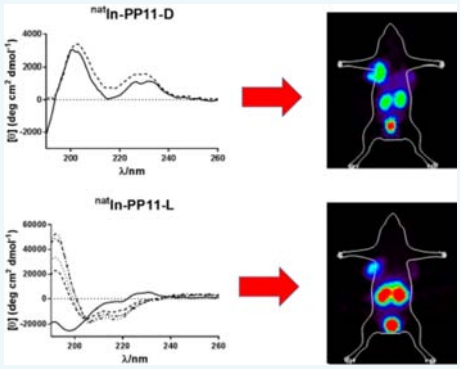

INTRODUCTION

Cholecystokinin-2 receptors (CCK2R) are (over)expressed in several tumor types, including medullary thyroid cancer (MTC), small cell lung cancer, astrocytomas, stromal ovarian cancer, gastroenteropancreatic tumors, and breast, endometrial, and ovarian adenocarcinomas.[1,2] Thus, CCK2R can be used as a target for corresponding radiolabeled peptide−minigastrin (MG, LEEEEEAYGWMDF-NH$_2$) analogues. These tumors can be visualized by imaging techniques, such as positron emission tomography (PET) and single photon emission computed tomography (SPECT), or treated with peptide−receptor radionuclide therapy (PRRT), if the peptide is labeled with a particle emitter. In recent years, clinical studies have emphasized the important role of gastrin receptor scintigraphy (GRS) for tumor detection in patients with metastatic MTC or neuroendocrine tumors when somatostatin receptor scintigraphy had failed.[3,4] It was recently demonstrated that cholecystokinin and MG analogues also bind to the CCK2R splice variant, CCK2i4sv, which is frequently expressed on gastrointestinal stromal tumors, insulinomas, and small cell lung cancer and not in normal tissue.[5,6] This opens additional possibilities for GRS and PRRT with MG analogues.

Although there are MG analogues suitable for GRS,[7−13] the best candidate for PRRT still needs to be found. Most radiolabeled MG analogues show good tumor uptake but at the same time very high kidney retention, which limits the maximal activity that can be administered without induction of radiation nephrotoxicity.[14] On the other hand, MG analogues with a reduced number of glutamic acid residues (reduced negative charge) show improved tumor-to-kidney ratios.[15] The drawback of truncated MG analogues is their low enzymatic stability in human serum,[15] which makes them poor candidates for clinical translation.[7,16] These findings indicate the important role of spacer length and chemical composition (charge) not only on kidney uptake but also on enzymatic stability.

High kidney retention of MG analogues has been related to N-terminal ionic glutamic acids residues and can be substantially reduced by coinjection of polyglutamic acids,[10] the gelatin-based plasma expander gelofusine,[17] or albumin and designated albumin fragments.[18] Our group recently showed

Received: April 8, 2015
Revised: May 8, 2015
Published: May 13, 2015

DOI: 10.1021/acs.bioconjchem.5b00187
Bioconjugate Chem. 2015, 26, 1113−1119

Table 1. Analytical Data of the Two Studied Minigastrin Analogues

code	amino acid sequence	HRMS calcd MW	HRMS obsvd MW	HPLC t_R (min)[a,b]
PP11−**D**	DOTA−(D-**Glu**)$_6$-Ala-Tyr-Gly-Trp-Met-Asp-Phe-NH$_2$	2047.80	2048.8080 $[M + H]^+$	15.65
PP11−**L**	DOTA−(L-**Glu**)$_6$-Ala-Tyr-Gly-Trp-Met-Asp-Phe-NH$_2$	2047.80	2048.8033 $[M + H]^+$	15.50
^{nat}In−PP11−**D**	^{nat}In−DOTA−(D-**Glu**)$_6$-Ala-Tyr-Gly-Trp-Met-Asp-Phe-NH$_2$	2160.80	2160.6857 $[M + H]^+$	16.32
^{nat}In−PP11−**L**	^{nat}In−DOTA−(L-**Glu**)$_6$-Ala-Tyr-Gly-Trp-Met-Asp-Phe-NH$_2$	2160.80	2160.6899 $[M + H]^+$	16.35

[a]Using an HPLC gradient system as described in the Experimental Section of the Supporting Information; t_R = retention time. [b]Purity was ≥95% in all cases.

that kidney retention can be highly reduced by exchanging ionic L-Glu in the MG sequence by the nonionic D-Gln isostere, which results in an increased tumor-to-kidney ratio and potentially a wider therapeutic window. At the same time, introduction of D-amino acid spacers resulted in a remarkable improvement in metabolic stability.[19] On the basis of circular dichroism (CD) measurements, it was hypothesized that the relatively stable secondary structure of the D-amino acid spacer analogue was most likely responsible for the high metabolic stability, together with its difficulty in adopting a conformation that easily fit into the active site of the corresponding enzymes, metallopeptidases.[19−22]

The difference in the secondary structure of the D-amino acid analogue prompted us to evaluate, in a comparative study, two minigastrin analogues that differ only in the stereochemistry of the spacer, namely, DOTA−(L-Glu)$_6$-Ala-Tyr-Gly-Trp-Met-Asp-Phe-NH$_2$ (PP11−**L**) and DOTA−(D-Glu)$_6$-Ala-Tyr-Gly-Trp-Met-Asp-Phe-NH$_2$ (PP11−**D**). The latter compound was found to be one of the most promising MG analogues for the detection of MTC in a multicenter study by the European COST action BM0607. In this study, we aim to better understand the relationship between the secondary structures of these peptides with the pharmacokinetics of the corresponding radiopharmaceuticals.

RESULTS

Synthesis and Radiolabeling. Peptides PP11−**D** and PP11−**L** were synthesized on solid phase using standard Fmoc chemistry. Purity was over 95%, as confirmed by RP-HPLC. Both the peptides and their metalated forms were characterized by HRMS and RP-HPLC (Table 1).

^{111}In labeling yields > 95% at specific activities > 37 GBq μmol^{-1} were achieved for both conjugates.

Binding Affinity Studies on CCK- and Gastrin Receptor-Expressing Tissues. The receptor binding affinities of the minigastrin analogues to cholecystokinin and gastrin receptor-positive tumor cells were determined and are expressed as IC_{50} values, which describes the concentration of the tested substance needed to inhibit the binding of ^{125}I−CCK by 50%. Corresponding IC_{50} values are listed in Table 2. Both metalated and nonmetalated compounds show comparable binding affinities; the IC_{50} values of PP11−**D** and ^{nat}In−PP11−**D** are 2.5- and 1.6-fold higher than the corresponding IC_{50} values of PP11−**L** and ^{nat}In−PP11−**L**.

Enzymatic Stability in Human Serum. Calculated half-lives of the radiolabeled minigastrin analogues in human blood serum were 175 ± 71 h for ^{111}In−PP11−**D** and 75 ± 23 h for ^{111}In−PP11−**L**. Introduction of 6 D-Glutamic acids in the MG analogue improved the serum stability more than 2-fold.

Circular Dichroism Spectroscopy. The CD spectra of ^{nat}In−PP11−**L** show two principal bands: one positive band around 225−230 nm and one negative band at 195 nm (Figure 1). This spectrum is characteristic of a random coil conformation, and the addition of TFE induced changes in the conformational preferences of the peptide, enhancing its propensity to assume an α-helical conformation. In contrast, the CD spectrum of ^{nat}In−PP11−**D** shows two positive bands at 195 and 225 nm and a weak negative band at 215 nm (Figure 1). We assigned this to a type II reverse turn conformation, based on model spectra for peptide secondary structure estimation reported by Reed et al.[23] The addition of 2,2,2-

Table 2. Binding Affinities toward CCKR and Calcium Mobilization Assay Results

code	IC_{50} (nmol L^{-1})[a] CCK1R	IC_{50} (nmol L^{-1})[a] CCK2R	EC_{50} (nmol L^{-1})[b]
PP11−**D**	>1000	1.8 ± 1.2 (3)	0.44
PP11−**L**	>1000	0.7 ± 0.2 (3)	0.32
^{nat}In−PP11−**D**		2.5 ± 1.4 (2)	
^{nat}In−PP11−**L**		1.5 ± 0.4 (2)	

[a]Binding affinities are expressed as IC_{50} values. The number of independent studies is listed in parentheses. [b]Calcium mobilization assay results are expressed as EC_{50} values, indicating the concentration at which 50% of the final effect is achieved.

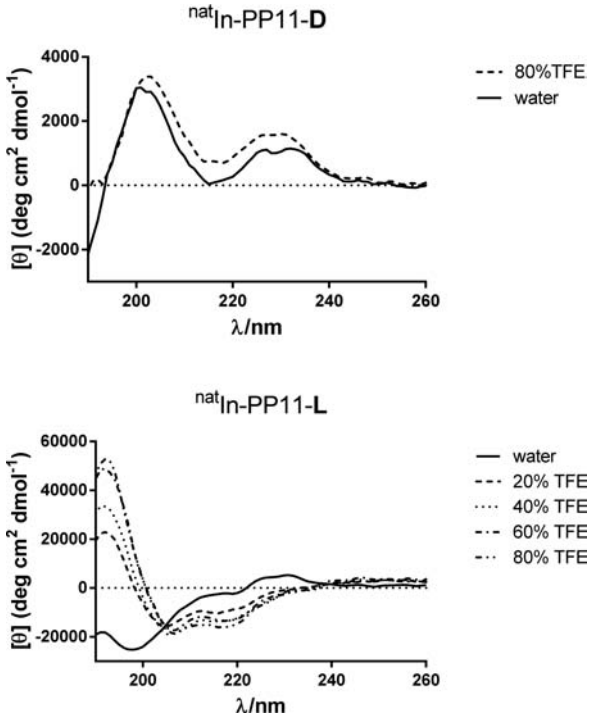

Figure 1. CD spectra of ^{nat}In−PP11−**D** and ^{nat}In−PP11−**L**.

DOI: 10.1021/acs.bioconjchem.5b00187
Bioconjugate Chem. 2015, 26, 1113−1119

trifluoroethanol (TFE) (80%) did not induce any changes in the secondary structure of the peptide.

Internalization Study. The fraction internalized by the AR4-2J cell line was evaluated and is expressed as the percent of added activity per 10^6 cells over a 4 h period (Figure 2). The

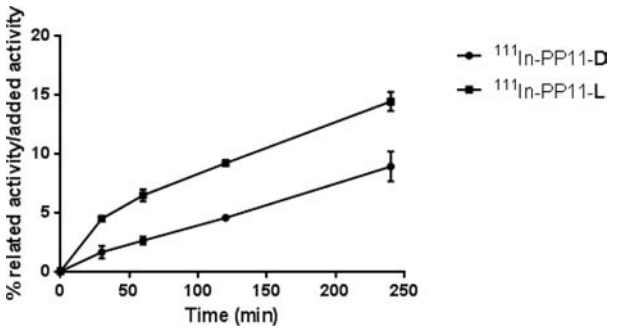

Figure 2. Internalization of ^{111}In−PP11−**D** and ^{111}In−PP11−**L** by the AR4-2J cell line (at 37 °C, 5% CO_2).

values at the designated time points significantly decreased to less than 0.5% after addition of excess unlabeled peptide ($p < 0.01$). The surface-bound radioligand did not exceed 1.5% of the added radioactivity after 4 h of incubation. The 4 h values of ^{111}In−PP11−**L** are 1.6-fold higher than the internalized fraction of ^{111}In−PP11−**D** (14.4 ± 0.8 vs 8.9 ± 1.3%).

Calcium Mobilization Assay. PP11−**D** and PP11−**L** were evaluated for their effect on signaling using a Ca^{2+} flux assay with AR4-2J cells. In the same assay, the antagonist proglumide was tested as a negative control (Figure 3). A sigmoidal dose−

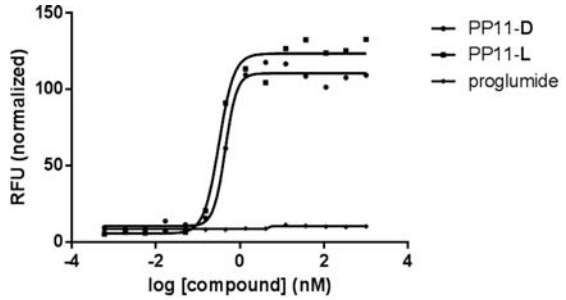

Figure 3. Intracellular calcium mobilization induced in AR4-2J cells by the two MG analogues (RFU, relative fluorescence units). Cells were loaded with Ca-dye and different concentrations of agonists starting from 1 μM. EC_{50} values were calculated using a four-parameter fitting equation (y = bottom + (top − bottom)/(1 + $10^{(\log EC_{50} - x \times \text{Hill Slope})}$)) with GraphPad Prism 5 sofware (La Jolla, CA).

response curve was obtained, indicating that the calcium response was dependent on peptide concentration. The EC_{50} value (Table 2) for PP11−**D** is slightly higher than the one calculated for PP11−**L** (0.44 and 0.32 nM, respectively). These values were calculated using a four-parameter fitting equation (Figure 3). As expected, no response was registered for the gastrin receptor antagonist proglumide.

Biodistribution Studies in AR4-2J Tumor-Bearing Lewis Rats. Biodistribution data of selected organs for both radiopeptides are summarized in Table 3. The full pharmacokinetic profile is reported in more detail in the Supporting Information (Table S1). Rapid clearance from all gastrin receptor-negative tissues and blood was observed. Uptake in gastrin receptor-rich tissues (stomach) as well as in the tumor was significantly reduced in animals preinjected with an excess of unlabeled peptides, indicating a specific receptor-mediated uptake. At 4 h postinjection (p.i.), ^{111}In−PP11−**D** shows tumor uptake 1.8-fold lower than that of ^{111}In−PP11−**L**. The washout from the tumor is faster for ^{111}In−PP11−**L** compared to that of ^{111}In−PP11−**D**. The kidneys are the main excretory pathway of these radiopeptides. ^{111}In−PP11−**D** shows a 23-fold lower kidney uptake compared to that of ^{111}In−PP11−**L**. In summary, at 4 h p.i., the tumor-to-kidney ratio for ^{111}In−PP11−**D** is improved 12-fold. The tumor-to-kidney ratio for ^{111}In−PP11−**D** remains 14-fold higher after 24 h p.i.

Preinjection of gelofusine to selected groups of animals further reduced the kidney retention of both radiopeptides. In the case of ^{111}In−PP11−**D**, a 2-fold reduction was observed, whereas in the case of ^{111}In−PP11−**L**, preinjection of gelofusine resulted in 95% kidney reduction.

Imaging Study. PET images of ^{68}Ga−PP11−**D** and ^{68}Ga−PP11−**L** were obtained on A431-CCK2R tumor-bearing nude mice at 1 h p.i. This particular animal/tumor model is often used in the literature to study gastrin receptor-binding peptides. Even though a different animal model and cell line, from that used in the biodistribution study, were used for the imaging study, the images mirror what was described for the ^{111}In study: comparable tumor uptake and much more pronounced kidney retention of the ^{68}Ga−PP11−**L** analogue (Figure 4).

DISCUSSION

There is currently no effective therapy available for patients with distant metastases of MTC. Radiopharmaceuticals suitable for PRRT should demonstrate high tumor uptake, tumor retention, and a favorable tumor-to-kidney ratio. The main problem facing most radiolabeled MG analogues is their high kidney retention, which has been related to the N-terminal glutamic acid sequence.[10,15,17] Chemical modification of MG analogues by eliminating charged glutamic acid residues demonstrated a positive correlation between low kidney uptake and retention and a decreasing number of negative charges.[15] Unfortunately, this change also distinctly decreased the enzymatic stability of the series of reported radiopeptides,[15] which makes them poor candidates for clinical use.[7] More recent approaches of exchanging the ionic -(L-Glu)$_6$- spacer with the nonionic -(D-Gln)$_6$- isostere resulted in highly reduced kidney retention and, at the same time, a remarkable improvement in enzymatic stability.[19] On the basis of CD measurements, it was hypothesized that the relatively stable secondary structure of the -(D-Gln)$_6$- isostere could be the reason for its high enzymatic stability as well as its difficulty in adopting a conformation that easily fits into the active site of the corresponding enzymes, such as zinc metallopeptidases ACE (angiotensin I-converting enzyme, EC 3.4.15.1.), which cleaves the penultimate peptide bond of short gastrins and releases the dipeptide Asp-Phe-NH_2, or the neutral peptidase (EC 3.4.24.11) with its major cleavage point between Asp and Phe.[19−22] This was a turning point for the present study. We decided to investigate a new minigastrin analogue in which the charge of the spacer is maintained (L-Glu$_6$) but the stereochemistry is changed (D-Glu$_6$). In fact, as presented herein, a CD study (Figure 1) shows that this change resulted in the same pattern as described above, with ^{nat}In−PP11−**D** having a relatively stable type II reverse turn conformation, which translates into higher enzymatic stability in human serum.

DOI: 10.1021/acs.bioconjchem.5b00187
Bioconjugate Chem. 2015, 26, 1113−1119

Table 3. Biodistribution Data of ^{111}In−PP11−D and ^{111}In−PP11−L along with Kidney Retention Blocking Using Gelofusine[a]

		^{111}In−PP11−D		^{111}In−PP11−L	
organ	time (h)	nonblocked	blocked[b]	nonblocked	blocked[b]
tumor	4	1.24 ± 0.43	0.22 ± 0.01	2.25 ± 0.23	0.58 ± 0.35
	24	0.63 ± 0.08		0.91 ± 0.41	
	4 + gelofusine[c]				
kidney	4	1.10 ± 0.23	2.12 ± 0.65	25.51 ± 2.58	24.86 ± 5.79
	24	0.87 ± 0.06		19.35 ± 5.58	
	4 + gelofusine[c]	0.52 ± 0.09		1.35 ± 0.63	
blood	4	0.01 ± 0.00	0.01 ± 0.00	0.01 ± 0.00	0.01 ± 0.00
	24	0.00 ± 0.00		0.01 ± 0.00	
	4 + gelofusine[c]	0.01 ± 0.00		0.01 ± 0.00	
liver	4	0.02 ± 0.01	0.05 ± 0.02	0.05 ± 0.01	0.04 ± 0.01
	24	0.01 ± 0.00		0.04 ± 0.01	
	4 + gelofusine[c]	0.02 ± 0.00		0.02 ± 0.00	
stomach	4	0.20 ± 0.10	0.03 ± 0.01	0.50 ± 0.03	0.12 ± 0.07
	24	0.17 ± 0.02		0.27 ± 0.10	
	4 + gelofusine[c]	0.16 ± 0.13		0.06 ± 0.04	
muscle	4	0.01 ± 0.01	0.02 ± 0.00	0.08 ± 0.02	0.07 ± 0.04
	24	0.01 ± 0.00		0.09 ± 0.02	
	4 + gelofusine[c]	0.01 ± 0.00		0.01 ± 0.00	
bone	4	0.28 ± 0.08	0.24 ± 0.09	0.25 ± 0.01	0.21 ± 0.09
	24	0.13 ± 0.03		0.27 ± 0.06	
	4 + gelofusine[c]	0.25 ± 0.02		0.13 ± 0.03	

tumor-to-tissue ratio	^{111}In−PP11−D (4 h/24 h p.i.)	^{111}In−PP11−L (4 h/24 h p.i.)
tumor/kidney	1.12/0.72	0.09/0.05
tumor/blood	205/625	171/159
tumor/stomach	6.2/3.8	4.5/3.4
tumor/liver	59/62	49.4/21.9
tumor/muscle	137/125	28/10
kidney/kidney gelofusine	2.1	19

[a]Uptake is given as the percentage of injected activity per gram of tissue (% IA g^{-1}), expressed as the mean value ± SD; 4 rats/group were used except for 4 h p.i. with ^{111}In−PP11−D, for which nine rats were used. [b]Blocked with 100 nmol of unlabeled (cold) peptide. [c]Preinjection of 20 mg of gelofusine (40 mg mL^{-1}, 500 μL per rat).

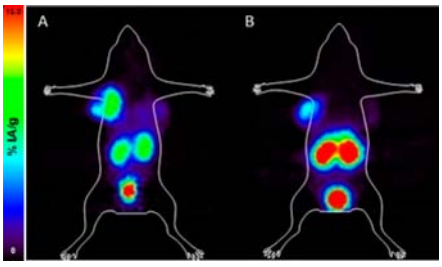

Figure 4. MicroPET scans of mice with subcutaneous A431-CCK2R tumors 1 h after injection of 5−7 MBq of ^{68}Ga-labeled PP11−D (A) and PP11−L (B). Radiotracer uptake is visible in the CCK2R tumors. A much more pronounced kidney retention of ^{68}Ga-labeled PP11−L can be clearly seen in the image (scale, 0−13% IA g^{-1}).

As shown (Tables 3 and S1), biodistribution studies of ^{111}In−PP11−D and ^{111}In−PP11−L in AR4-2J tumor-bearing Lewis rats revealed that the pharmacokinetics of the radiopeptide changes by maintaining the overall charge of the molecule and changing just the stereochemistry of the amino acid spacer. The tumor uptake is nearly 2-fold higher in the case of ^{111}In−PP11−L, which reflects its higher binding affinity, lower EC_{50}, and consequently higher internalization rate compared to those of PP11−D (Table 2 and Figures 2 and 3). However, the most pronounced difference was observed in the kidney uptake and retention of both radiopeptides, which is in contrast to literature reports regarding the positive correlation between the charge of the molecule and its retention in the kidneys.[15,17] Consequently, the tumor-to-kidney ratio for ^{111}In−PP11−D 4 h p.i. is improved 12-fold and also remains high after 24 h p.i.

It has been shown that the mechanism of (radio)peptides accumulation in the kidneys is mediated by amino acid transport systems.[24,25] Gotthardt et al.[17] investigated the inhibition of renal accumulation of different classes of radiopeptides, i.e., octreotide, MG, glucagon-like peptide-1 (exendin), and bombesin, using Lys, gelofusine, or polyglutamic acid. Inhibiting the renal accumulation of the tested radiopeptides could be achieved by either Lys or PGA, suggesting that there are two different uptake mechanisms. Interestingly, gelofusine was shown to be the only compound that inhibited the renal accumulation of all radiopeptides tested, indicating the existence of another mechanism or its action on both mechanisms mentioned above. Gelofusine is succinylated gelatin, used as a plasma expander, which causes low-molecular weight proteinuria. It was postulated that this effect is most likely due to competitive inhibition of tubular protein reabsorption.[26]

With this in mind, we explored the possibility of further improving the tumor-to-kidney ratio of ^{111}In−PP11−D using gelofusine. As shown (Tables 3 and S1), by preinjecting gelofusine to selected groups of animals, the extent of the reduction in kidney uptake and retention of ^{111}In−PP11−D and ^{111}In−PP11−L unexpectedly differs by almost 10-fold. We

DOI: 10.1021/acs.bioconjchem.5b00187
Bioconjugate Chem. 2015, 26, 1113−1119

propose that the difference in kidney retention and in gelofusine efficiency in kidney protection for both radiopeptides may be related to differences in their secondary structure and, hence, different uptake mechanisms for both radiopeptides, as suggested already by the study of Gotthardt et al.[17] It is known from the literature that the scavenger receptor megalin plays an important role in the renal reabsorption of different radiopeptides.[27] Since megalin contains four large binding domains, gelofusine and ^{111}In−PP11−**L** could have a preference for binding to the same domain, whereas ^{111}In−PP11−**D** does not. We postulate that the large difference in the extent of kidney blocking by gelofusine could be directly related to the difference in enzymatic stability in the kidneys. In this respect, the possibly higher blocking potency of gelofusine toward shorter metabolites of ^{111}In−PP11−**L** (having a higher negative charge density) could explain the difference of 95% versus the 50%. Ongoing studies of kidney uptake using metabolites may prove the adequacy of this hypothesis.

Even though the kidney retention of ^{111}In−PP11−**D** is 20-fold lower than that of ^{111}In−PP11−**L**, a direct comparison of the kidney retention and uptake for these analogues with those of the nonionic -(D-Gln)$_6$- isostere studied in our previous work[19] still shows the contribution of the charge to the retention in the kidneys (1.10 ± 0.23% IA g^{-1} vs 0.33 ± 0.05% IA g^{-1} at 4 h p.i.; the same animal and tumor model was used as well as the same peptide quantity as that used herein). Since preinjecting gelofusine results in a drop in kidney retention to 0.52 ± 0.09% IA g^{-1}, we postulate that most of the contribution of charge to uptake in the kidneys is blocked by gelofusine. Thus, this remaining activity in the kidneys is most probably due to another uptake mechanism, such as fluid-phase endocytosis.

The comparable tumor uptake and large difference in kidney retention of these analogues were also observed in a microPET imaging study performed with either ^{68}Ga−PP11−**D** or ^{68}Ga−PP11−**L** using a different animal model and cell line. In contrast to the biodistribution experiments, the imaging studies were performed in the same animal model and cell line used in previous studies evaluating minigastrin analogues in vivo,[28] indicating that species differences are not responsible for the observed effect.

In summary, we have presented two isomeric molecules, with the same chemical composition and charge, that differ only in the stereochemistry of the amino acids that form the spacer. They present with similar binding affinity, internalization profile, and value for Ca^{2+} mobilization (EC_{50}; Table 2). They show a difference in their enzymatic stability and a large difference in their kidney uptake and retention. Additionally, the nephroprotective agent gelofusine reduces their kidney uptake and retention to differing extents. In the present study, we demonstrated that high kidney retention and uptake are not determined solely by the charge of the ligand but also by the secondary structure of the peptide. This observation is in striking contrast with the generally accepted hypothesis in the literature that the charge of the ligand determines its retention in the kidneys.[15,17] New, carefully controlled studies are warranted to confirm our hypothesis of the influence of secondary structure on the pharmacokinetics of the selected radiopeptides. This could provide valuable new insight into the mechanism of kidney uptake and retention of small radiopeptides.

EXPERIMENTAL SECTION

Chemicals. The supplier information for all of the reagents, radionuclides, and generator as well as details of the instruments used is provided in the Supporting Information.

Cell Lines. AR4-2J rat pancreatic tumor cells were obtained from ATCC (Virginia, USA) and cultured as described previously.[15]

A431-CCK2R transfected cells were kindly provided by Dr. Aloj (Fondazione 'G. Pascale', Naples, Italy) and cultured as described previously.[29]

Synthesis. The peptide−chelator conjugates were synthesized manually by a standard Fmoc strategy, using Rink amide MBHA resin, as described in the Supporting Information. The peptides were purified by semipreparative RP-HPLC, analyzed by analytical RP-HPLC, and characterized by HRMS.

Peptides PP11−**D** and PP11−**L** were complexed with $^{nat}InCl_3$ using the procedure described in the Supporting Information. The pure product, obtained as white powder after lyophilization, was analyzed by analytical HPLC and characterized using HRMS.

Preparation of the Radiotracer. ^{111}In− and ^{68}Ga−DOTA−peptide conjugates were prepared as described in detail in the Supporting Information and elsewhere.[30]

Binding Affinity Studies on Cholecystokinin-1- or Cholecystokinin-2-Expressing Tissues. Binding affinities were evaluated as described[11] in surgically resected human tumor tissues selected from previous experiments to express either CCK1 or gastrin receptor.[1] Increasing amounts of minigastrin derivatives were added to the ^{125}I−D-Tyr-Gly-Asp-Tyr(SO$_3$H)-Nle-Gly-Trp-Nle-Asp-Phe-NH$_2$ (^{125}I−CCK) containing incubation medium to generate competitive inhibition curves. Tissue slides were exposed to Biomax MR films (Kodak) for 7 days. Autoradiograms were quantified using tissue standards for iodinated compounds (Amersham, UK).[31,32]

Enzymatic Stability in Human Serum. Enzymatic stability of ^{111}In-labeled peptides was performed following the protocol described in the Supporting Information and earlier.[19]

Circular Dichroisms Spectroscopy. The CD measurements were performed at 25 °C using a Chirascan spectrometer (Applied Photophysics Ltd., UK). The instrument was purged with nitrogen gas at 20 L min^{-1} for 20 min before and during measurements. All spectra were recorded from 260 to 185 nm using a spectral bandwidth of 1 nm at 25 °C with a time constant of 3 s and a step resolution of 1 nm. CD data are given as mean residual molar ellipticities (Θ in mdeg cm^2 dmol^{-1}). A Quartz cell with a path length of 1 cm was used. The peptides were dissolved in H_2O in order to obtain a concentrated solution of 0.4 mM, which was then diluted to obtain the concentration required for the CD experiment (40 μM). Samples' spectra were recorded after adding different percentages of TFE and different solvents.

Internalization Studies with the AR4-2J Cell Line. AR4-2J cells were seeded at a density of 0.5−1.0 × 10^6 cells per well in 6-well plates and incubated overnight to obtain good cell adherence. On the day of the experiment, cells were treated exactly as described recently.[33]

Calcium Mobilization Assay. Intracellular calcium mobilization was measured in AR4-2J cells using the calcium 3 assay kit (Molecular Probes, Inc.) following the protocol described in the Supporting Information and earlier.[19,34]

DOI: 10.1021/acs.bioconjchem.5b00187
Bioconjugate Chem. 2015, 26, 1113−1119

Biodistribution Experiments in AR4-2J Tumor-Bearing Lewis Rats. All animal experiments were performed in compliance with the Swiss regulation for animal treatment (permit no. 789) and the guidelines of the German Law for the Use of Living Animals in Scientific Studies. Lewis male rats were implanted subcutaneously with 10^7 AR4-2J tumor cells, which were freshly expanded, in sterilized phosphate-buffered saline (PBS, pH 7.4) solution. Eleven to 16 days after inoculation (tumor mass, 1.6−3.7 g), the rats' tail veins were injected with 0.1 nmol of ^{111}In-radiolabeled peptide (about 1.1 MBq, dissolved in 200 μL of 0.9% NaCl solution). For the determination of nonspecific uptake in tumor or receptor positive organs, a group of animals was coinjected with 100 nmol of unlabeled peptide in 0.9% NaCl solution. To reduce kidney uptake, gelofusine (40 mg/mL) was preinjected (5 min) into Lewis male rats (500 μL per rat).

At 4 and 24h p.i., the rats were sacrificed, and organs of interest were collected, rinsed of excess blood, blotted dry, weighed, and counted in a γ-counter. The total counts injected per animal were determined by extrapolation from counts of an aliquot taken from the injected solution as a standard. The uptake in different organs was calculated as the percentage of injected activity per gram tissue (% IA g^{-1}).

Imaging Study. Female nude mice were subcutaneously implanted with 5×10^6 A431-CCK2R cells. The experiment was performed 10 days after implantation (tumor weight, 0.2−0.4 g). MicroPET scans were performed using a dedicated small-animal PET scanner (Focus 120 microPET scanner; Concorde Microsystems Inc.). About 150 pmol/100 μL of ^{68}Ga−PP11−**D** and ^{68}Ga−PP11−**L** (5−7 MBq) was intravenously injected into the tail vein.

Animals were anesthetized with 1.5% isoflurane, and static scans were acquired at 1 h p.i., for 30 min. PET images were reconstructed with filtered back projection. No correction was applied for attenuation. Images were generated using AMIDE software (25). The color scale was set from 0−13% IA g^{-1} to allow for qualitative comparison among the images.

Statistical Methods. Data are expressed as mean ± standard deviation, which were calculated using Microsoft Excel. To compare differences between groups, Student's t test was used. p values < 0.01 were considered to be statistically significant. Origin 7.5 software (Microcal Software, Inc.) was used to fit a first-order decay model for calculating serum half-life values.

■ ASSOCIATED CONTENT

Supporting Information

Additional data on chemicals, synthesis, characterization, and evaluation of the two (radio)peptides, ^{111}In−PP11−**D** and ^{111}In−PP11−**L**; extended table of biodistribution results of PP11−**D** and ^{111}In−PP11−**L**. The Supporting Information is available free of charge on the ACS Publications website at DOI: 10.1021/acs.bioconjchem.5b00187.

■ AUTHOR INFORMATION

Corresponding Author

*E-mail: rosalba.mansi@usb.ch.

Notes

The authors declare no competing financial interest.

■ ACKNOWLEDGMENTS

We thank Prof. H. Wennemers and Dr. M. Kümin for support with the CD measurements, Dr. M. Behe for valuable scientific discussion, Novartis Pharma for analytic assistance, S. Tschumi for expert technical help, and the COST BM0607 action and Colonview (Früherkennung und intraoperative Lokalisation des Kolonkarzinoms) for financial support.

■ ABBREVIATIONS

CCK2, cholecystokinin2; GIST, gastrointestinal stromal tumor; DOTA, 1,4,7,10-tetraazacyclododecane-1,4,7,10-tetraacetic acid; HRMS, high-resolution mass spectrometry; RP-HPLC, reversed-phase high-performance liquid chromatography; TFE, 2,2,2-trifluoroethanol; PBS, phosphate buffer saline; IA g^{-1}, injected activity per gram of tissue

■ REFERENCES

(1) Reubi, J. C., Schaer, J. C., and Waser, B. (1997) Cholecystokinin-(CCK)-A and CCK-B/gastrin receptors in human tumors. *Cancer Res. 57*, 1377−1386.

(2) Reubi, J. C., and Waser, B. (1996) Unexpected high incidence of cholecystokinin-B/gastrin receptors in human medullary thyroid carcinomas. *Int. J. Cancer 67*, 644−647.

(3) Gotthardt, M., Behe, M. P., Beuter, D., Battmann, A., Bauhofer, A., Schurrat, T., Schipper, M., Pollum, H., Oyen, W. J., and Behr, T. M. (2006) Improved tumour detection by gastrin receptor scintigraphy in patients with metastasised medullary thyroid carcinoma. *Eur. J. Nucl. Med. Mol. Imaging 33*, 1273−1279.

(4) Gotthardt, M., Behe, M. P., Grass, J., Bauhofer, A., Rinke, A., Schipper, M. L., Kalinowski, M., Arnold, R., Oyen, W. J., and Behr, T. M. (2006) Added value of gastrin receptor scintigraphy in comparison to somatostatin receptor scintigraphy in patients with carcinoids and other neuroendocrine tumours. *Endocr.-Relat. Cancer 13*, 1203−1211.

(5) Korner, M., Waser, B., Reubi, J. C., and Miller, L. J. (2010) CCK_2 receptor splice variant with intron 4 retention in human gastrointestinal and lung tumours. *J. Cell. Mol. Med. 14*, 933−943.

(6) Laverman, P., Roosenburg, S., Gotthardt, M., Park, J., Oyen, W. J., de Jong, M., Hellmich, M. R., Rutjes, F. P., van Delft, F. L., and Boerman, O. C. (2008) Targeting of a CCK_2 receptor splice variant with ^{111}In-labelled cholecystokinin-8 (CCK8) and ^{111}In-labelled minigastrin. *Eur. J. Nucl. Med. Mol. Imaging 35*, 386−392.

(7) Froberg, A. C., de Jong, M., Nock, B. A., Breeman, W. A., Erion, J. L., Maina, T., Verdijsseldonck, M., de Herder, W. W., van der Lugt, A., Kooij, P. P., and Krenning, E. P. (2009) Comparison of three radiolabelled peptide analogues for CCK-2 receptor scintigraphy in medullary thyroid carcinoma. *Eur. J. Nucl. Med. Mol. Imaging 36*, 1265−1272.

(8) Laverman, P., Behe, M., Oyen, W. J., Willems, P. H., Corstens, F. H., Behr, T. M., and Boerman, O. C. (2004) Two technetium-99m-labeled cholecystokinin-8 (CCK8) peptides for scintigraphic imaging of CCK receptors. *Bioconjugate Chem. 15*, 561−568.

(9) Mather, S. J., McKenzie, A. J., Sosabowski, J. K., Morris, T. M., Ellison, D., and Watson, S. A. (2007) Selection of radiolabeled gastrin analogs for peptide receptor-targeted radionuclide therapy. *J. Nucl. Med. 48*, 615−622.

(10) Nock, B. A., Maina, T., Behe, M., Nikolopoulou, A., Gotthardt, M., Schmitt, J. S., Behr, T. M., and Macke, H. R. (2005) CCK-2/gastrin receptor-targeted tumor imaging with ^{99m}Tc-labeled minigastrin analogs. *J. Nucl. Med. 46*, 1727−1736.

(11) Reubi, J. C., Waser, B., Schaer, J. C., Laederach, U., Erion, J., Srinivasan, A., Schmidt, M. A., and Bugaj, J. E. (1998) Unsulfated DTPA− and DOTA−CCK analogs as specific high-affinity ligands for CCK-B receptor-expressing human and rat tissues in vitro and in vivo. *Eur. J. Nucl. Med. 25*, 481−490.

(12) von Guggenberg, E., Behe, M., Behr, T. M., Saurer, M., Seppi, T., and Decristoforo, C. (2004) ^{99m}Tc-labeling and in vitro and in vivo

DOI: 10.1021/acs.bioconjchem.5b00187
Bioconjugate Chem. 2015, 26, 1113−1119

evaluation of HYNIC- and (Nalpha-His)acetic acid-modified [D-Glu1]−minigastrin. *Bioconjugate Chem. 15*, 864−871.
(13) von Guggenberg, E., Dietrich, H., Skvortsova, I., Gabriel, M., Virgolini, I. J., and Decristoforo, C. (2007) ^{99m}Tc-labelled HYNIC-minigastrin with reduced kidney uptake for targeting of CCK-2 receptor-positive tumours. *Eur. J. Nucl. Med. Mol. Imaging 34*, 1209−1218.
(14) Behe, M., and Behr, T. M. (2002) Cholecystokinin-B (CCK-B)/gastrin receptor targeting peptides for staging and therapy of medullary thyroid cancer and other CCK-B receptor expressing malignancies. *Biopolymers 66*, 399−418.
(15) Good, S., Walter, M. A., Waser, B., Wang, X., Muller-Brand, J., Behe, M. P., Reubi, J. C., and Maecke, H. R. (2008) Macrocyclic chelator-coupled gastrin-based radiopharmaceuticals for targeting of gastrin receptor-expressing tumours. *Eur. J. Nucl. Med. Mol. Imaging 35*, 1868−1877.
(16) Breeman, W. A., Froberg, A. C., de Blois, E., van Gameren, A., Melis, M., de Jong, M., Maina, T., Nock, B. A., Erion, J. L., Macke, H. R., and Krenning, E. P. (2008) Optimised labeling, preclinical and initial clinical aspects of CCK-2 receptor-targeting with 3 radiolabeled peptides. *Nucl. Med. Biol. 35*, 839−849.
(17) Gotthardt, M., van Eerd-Vismale, J., Oyen, W. J., de Jong, M., Zhang, H., Rolleman, E., Maecke, H. R., Behe, M., and Boerman, O. (2007) Indication for different mechanisms of kidney uptake of radiolabeled peptides. *J. Nucl. Med. 48*, 596−601.
(18) Vegt, E., van Eerd, J. E., Eek, A., Oyen, W. J., Wetzels, J. F., de Jong, M., Russel, F. G., Masereeuw, R., Gotthardt, M., and Boerman, O. C. (2008) Reducing renal uptake of radiolabeled peptides using albumin fragments. *J. Nucl. Med. 49*, 1506−1511.
(19) Kolenc-Peitl, P., Mansi, R., Tamma, M., Gmeiner-Stopar, T., Sollner-Dolenc, M., Waser, B., Baum, R. P., Reubi, J. C., and Maecke, H. R. (2011) Highly improved metabolic stability and pharmacokinetics of indium-111-DOTA−gastrin conjugates for targeting of the gastrin receptor. *J. Med. Chem. 54*, 2602−2609.
(20) Dubreuil, P., Fulcrand, P., Rodriguez, M., Fulcrand, H., Laur, J., and Martinez, J. (1989) Novel activity of angiotensin-converting enzyme. Hydrolysis of cholecystokinin and gastrin analogues with release of the amidated C-terminal dipeptide. *Biochem. J. 262*, 125−130.
(21) Dubreuil, P., Fulcrand, P., Rodriguez, M., Laur, J., Bali, J. P., and Martinez, J. (1990) ACE-like hydrolysis of gastrin analogs and CCK-8 by fundic mucosal cells of different species with release of the amidated C-terminal dipeptide. *Biochim. Biophys. Acta 1039*, 171−176.
(22) Roques, B. P., Noble, F., Dauge, V., Fournie-Zaluski, M. C., and Beaumont, A. (1993) Neutral endopeptidase 24.11: structure, inhibition, and experimental and clinical pharmacology. *Pharmacol. Rev. 45*, 87−146.
(23) Reed, J., and Reed, T. A. (1997) A set of constructed type spectra for the practical estimation of peptide secondary structure from circular dichroism. *Anal. Biochem. 254*, 36−40.
(24) Behr, T. M., Sharkey, R. M., Sgouros, G., Blumenthal, R. D., Dunn, R. M., Kolbert, K., Griffiths, G. L., Siegel, J. A., Becker, W. S., and Goldenberg, D. M. (1997) Overcoming the nephrotoxicity of radiometal-labeled immunoconjugates: improved cancer therapy administered to a nude mouse model in relation to the internal radiation dosimetry. *Cancer 80*, 2591−2610.
(25) van Eerd, J. E., Vegt, E., Wetzels, J. F., Russel, F. G., Masereeuw, R., Corstens, F. H., Oyen, W. J., and Boerman, O. C. (2006) Gelatin-based plasma expander effectively reduces renal uptake of ^{111}In-octreotide in mice and rats. *J. Nucl. Med. 47*, 528−533.
(26) ten Dam, M. A., Branten, A. J., Klasen, I. S., and Wetzels, J. F. (2001) The gelatin-derived plasma substitute gelofusine causes low-molecular-weight proteinuria by decreasing tubular protein reabsorption. *J. Crit. Care 16*, 115−120.
(27) Vegt, E., Melis, M., Eek, A., de Visser, M., Brom, M., Oyen, W. J., Gotthardt, M., de Jong, M., and Boerman, O. C. (2011) Renal uptake of different radiolabelled peptides is mediated by megalin: SPECT and biodistribution studies in megalin-deficient mice. *Eur. J. Nucl. Med. Mol. Imaging 38*, 623−632.
(28) Laverman, P., Joosten, L., Eek, A., Roosenburg, S., Peitl, P. K., Maina, T., Macke, H., Aloj, L., von Guggenberg, E., Sosabowski, J. K., de Jong, M., Reubi, J. C., Oyen, W. J., and Boerman, O. C. (2011) Comparative biodistribution of 12 ^{111}In-labelled gastrin/CCK2 receptor-targeting peptides. *Eur. J. Nucl. Med. Mol. Imaging 38*, 1410−1416.
(29) Aloj, L., Caraco, C., Panico, M., Zannetti, A., Del Vecchio, S., Tesauro, D., De Luca, S., Arra, C., Pedone, C., Morelli, G., and Salvatore, M. (2004) In vitro and in vivo evaluation of ^{111}In-DTPAGlu-G-CCK8 for cholecystokinin-B receptor imaging. *J. Nucl. Med. 45*, 485−494.
(30) Fani, M., Mueller, A., Tamma, M. L., Nicolas, G., Rink, H. R., Cescato, R., Reubi, J. C., and Maecke, H. R. (2010) Radiolabeled bicyclic somatostatin-based analogs: a novel class of potential radiotracers for SPECT/PET of neuroendocrine tumors. *J. Nucl. Med. 51*, 1771−1779.
(31) Erchegyi, J., Cescato, R., Grace, C. R., Waser, B., Piccand, V., Hoyer, D., Riek, R., Rivier, J. E., and Reubi, J. C. (2009) Novel, potent, and radio-iodinatable somatostatin receptor 1 (sst1) selective analogues. *J. Med. Chem. 52*, 2733−2746.
(32) Reubi, J. C., Kvols, L. K., Waser, B., Nagorney, D. M., Heitz, P. U., Charboneau, J. W., Reading, C. C., and Moertel, C. (1990) Detection of somatostatin receptors in surgical and percutaneous needle biopsy samples of carcinoids and islet cell carcinomas. *Cancer Res. 50*, 5969−5977.
(33) Zhang, H., Chen, J., Waldherr, C., Hinni, K., Waser, B., Reubi, J. C., and Maecke, H. R. (2004) Synthesis and evaluation of bombesin derivatives on the basis of pan-bombesin peptides labeled with indium-111, lutetium-177, and yttrium-90 for targeting bombesin receptor-expressing tumors. *Cancer Res. 64*, 6707−6715.
(34) Cescato, R., Maina, T., Nock, B., Nikolopoulou, A., Charalambidis, D., Piccand, V., and Reubi, J. C. (2008) Bombesin receptor antagonists may be preferable to agonists for tumor targeting. *J. Nucl. Med. 49*, 318−326.

DOI: 10.1021/acs.bioconjchem.5b00187
Bioconjugate Chem. 2015, 26, 1113−1119